TITLE: Flow Patterns in a Slurry-Bubble-Column Reactor Under Reaction Conditions

PI (AUTHORS): B. A. Toseland, D. M. Brown, B. S. Zou, M. P. Dudukovic

INSTITUTION/ORGANIZATION: Air Products and Chemicals, Inc.
Washington University, St. Louis

CONTRACT NUMBER: DE-FC22-94PC93052

PERIOD OF PERFORMANCE: June 1994 — August 1995

OBJECTIVE: Understand Flow Patterns in SCBB

ABSTRACT

The gas and liquid radioactive tracer response curves obtained in an industrial bubble column reactor of height to diameter ratio of 10 are analyzed and the suitability of the axial dispersion model for interpretation of the results is discussed. The relationship between the tracer concentration distribution and measured detector response is calculated. It is found that the liquid can be considered well mixed and that the response of the soluble gas tracer (Ar-41) is possibly dominated by the dissolved gas. The one dimensional axial dispersion model cannot match all the experimental observations well and the flow pattern of the undissolved gas cannot be determined with certainty.

INTRODUCTION

Radioactive tracers have been used to study flow and mixing in bubble columns (Field and Davidson, 1980; Air Products and Chemicals, 1990; Tarmy et al., 1982; Nalitham and Davies, 1987). Model-supported interpretation of tracer data allows extraction of parameters for design and scale up and is a necessary addition to visual inspection of data. The axial dispersion model is most frequently used for interpreting tracer data. The above cited studies either ignore gas absorption or assume that the gas tracer is instantaneously equilibrated between the gas and the liquid phase. The standard gas-phase model, however, needs modification to account for gas solubility (Joseph and Shah, 1986). Moreover, Vermeer and Krishna (1981) demonstrated the presence of a bi-modal bubble size distribution in the churn- turbulent regime. This distribution is not accounted for in the dispersion type model. However, no general model that can be fitted to tracer data was presented. Shetty and Kantak (1992) developed a two-bubble-class model and matched some data reported in the literature. Unfortunately, their model requires a large number of independently measured parameters which were not available in the present study.

The purpose of this study was to scrutinize the tracer data collected while conducting a reaction in a 0.57 m i.d. bubble-column, assess the extent of backmixing in the liquid and gas phases, and test the ability of the models to consistently match experimental observations. Dispersion models, being the simplest and most popular, were tried first. Follow-up work will use other models. A simple model for radiation measurements is also discussed to assess the errors in measuring tracer curves.

EXPERIMENTAL

The Alternate Fuels Development Unit (AFDU) at LaPorte, Texas owned by the United States Department of Energy (DOE) is a stainless steel bubble-column reactor with an internal diameter of 0.57 m and a possible liquid height of 7.62 m (Air Products and Chemicals, 1990). The stationary slurry phase is a powdered catalyst suspended in

a hydrocarbon oil. Gas bubbles through the slurry via a sparger. Oil disengages from the gas in a space above the liquid, and gas exits from the reactor through the top of the column.

The tracer curves were measured by ICI TracerCo of Houston, Texas. Ar-41, used as the gas phase tracer, was introduced into the feed line upstream of the vessel. Tests were performed in a reacting system. Manganese oxide was the liquid tracer since the particle size ($< 45\mu m$) was small enough to mimic the liquid flow (Air Products and Chemicals, 1990).

The flow distribution within the reactor was monitored by four rings of four detectors. The four detectors of each ring are evenly distributed around the circumference of the reactor. Detector rings were located at 30.5 cm, 149.9 cm, 337.8 cm and 482.6 cm vessel elevations. The liquid level during tracer studies was at 546.1 cm elevation. During the vapor studies, additional detectors were placed on the feed inlet and reactor overhead piping. During the liquid studies these detectors were repositioned at 200.7 cm and 292.1 cm elevations.

The reactor temperature was 300 $°C$, pressure was 2.7 atm. The reaction was the dehydration of isobutanol to isobutylene and water. Conversion was nearly complete so that the number of moles of gas almost doubled in the reactor. Gas holdup data taken by means of nuclear density gauge clearly shows the effect of the expanding gas flow. The particular example used later has a superficial gas velocity of 7.01 cm/s and an average gas holdup of 0.20.

INTERPRETATION OF TRACER DATA

The residence time distribution (RTD) theory (Duduković, 1986; Nauman, 1987) suggests that the parameters of a suitable model be found by minimizing some measure of the error between model predictions and experimental data. Closed form expressions for the most popular models for the impulse response mixing cup concentration at the reactor outlet are available to be matched to the data. The difficulties with interpreting industrial data arise mainly from two factors: 1) tracer input is not always an instantaneous pulse or it is not made at the reactor inlet; 2) measurements do not capture the mixing cup concentration and are often performed on the reactor itself, not at its outlet. Finally, the model may be too simplistic in nature to match all of the observed features. Space limitations do not allow us to address all of the above issues here. It may be noted that in this study the duration of the tracer injection was of the order of a few seconds, so that the input can be considered instantaneous. The relationship between radiation measurements and tracer concentration is discussed below because this important issue seems to be overlooked in the studies reported so far.

Distortions due to Radiation Measurements

The radiation signals measured by the scintillation detectors are affected by the solid angle subtended by the cylindrical detector, the distance between the radiation source and the detector, the attenuation and buildup factors (Tsouflanidis, 1983). Establishing the relationship between the measured radiation signals and the instantaneous three dimensional concentration distribution of the emitting tracer can only be done via tomography. However, the spatial range from which a detector receives most of its signal can be assessed. We consider a single detector in the bubble column and assume a uniform tracer distribution throughout the column, as is the case at the end of the liquid tracer

experiment.

The schematic is shown in Fig. 1. The bubble column is considered as divided into many compartments. The radiation from each compartment which is received by the detector is calculated. We denote d_M as the distance traveled through the gas-liquid mixture, d_S as the distance through stainless steel and d_A as the distance through air. We assume that the detector receives the radiation signal both on its front flat circular face (diameter = 5.1 cm) and on the cylindrical side face (length = 5.1 cm).

The total detector counting rate resulting from a point source inside the bubble column is:

$$N_t = e^{-\mu_M d_M}(1 + a_1\mu_M d_M e^{b_1\mu_M d_M})e^{-\mu_S d_S}(1 + a_2\mu_S d_S e^{b_2\mu_S d_S})\frac{A\epsilon S}{4\pi(d_M + d_S + d_A)^2} \quad (1)$$

where A is the area of the part of the detector which can be directly irradiated by the point source, ϵ is the detector efficiency. Other symbols are defined in the nomenclature, together with their default values.

The results of the radiation calculation are also shown in Fig. 1. The calculated radiation measurement is normalized so that the radiation measurement from the closest compartment equals to 1. The recorded intensity from a compartment which is 38 cm away from the detector is less than 1% of the recorded intensity from the closest compartment, with the source strength being the same. Those compartments whose distances from the detector are less than 56 cm contribute 90% of the total radiation intensity so that the large number of compartments far away form the detector do no swamp the signal.

Only the response of the detectors located around the vessel outlet pipe is approximately proportional to the tracer cross sectional average concentration. The signals received by the detectors located around the vessel (see Fig. 1) are mainly proportional to the amount of tracer present in a hemisphere about 15.2 cm in radius centered at the flat face of the detector. The detectors in the study were shielded on the sides, i.e., partially collimated, but the basic conclusion that the region close to the detector face influences the response most still holds. One can also show that the radiation signal at a given elevation is broader than the corresponding cross sectional concentration at the same elevation. This broadening is severe for systems close to plug flow and nonexistent for a completely back-mixed system. Since, as will be shown below, our bubble column is well mixed, this broadening is not a major factor.

Liquid Tracer

Liquid tracer is introduced at the 175.3 cm elevation close to the reactor wall at one side of the column. Detector responses at all elevations indicate lack of symmetry in the response which is the least severe at the 482.6 cm elevation. Therefore, the model prediction is fitted to the normalized response at 482.6 cm elevation. A one dimensional dispersion, with a constant dispersion coefficient in a batch liquid, is assumed with instantaneous tracer injection at the 175.3 cm elevation and cross-sectional average concentration measurement at the 482.6 cm elevation.

The liquid phase dispersion coefficient was obtained by matching the model predicted response to the detector response at the 482.6 cm elevation and a value of D_L=3,244 (cm^2/s) was found to yield the best fit. Figure 2 shows that the match between the model and data is reasonable. The dispersion coefficient of 3,244 (cm^2/s) at the inlet gas superficial velocity of 7 (cm/s) is about twice as large as the values predicted by typical

correlations (Fan, 1989) for the same diameter column. Since gas volume doubles due to reaction, liquid dispersion coefficients of the order of 2,000 (cm^2/s) are predicted by correlations at the doubled inlet superficial gas velocity. It is possible that additional liquid backmixing arises from in-situ gas generation.

The large value of the liquid dispersion coefficient indicates that the liquid is almost completely mixed. The characteristic liquid mixing time is of the order $L^2/D_L = 92$ seconds. Figure 2 also indicates that liquid mixing is complete in about 1.5 minutes.

Gas Tracer

A thorough literature search was carried out to locate transient models which deal with churn-turbulent regime of operation of bubble columns. It is found that no model is readily applicable to our tracer data, for the reason that either the model is incomplete or the required data is incomplete. Since the axial dispersion model with interphase mass transfer can to some extent simulate the behavior of bimodal bubble size distribution in churn turbulent regime by assuming that the small bubbles behave the same as the adsorbed tracer, this model is chosen as our first attempt to quantify the tracer data.

Gas tracer is introduced in the inlet pipe and monitored at the wall along the reactor length and in the exit pipe. Our task was to determine whether a one dimensional dispersion model can fit the observed measurements along the reactor length. Versions of the dispersion model that assumed equilibration between gas and liquid or a completely backmixed liquid were unable to match the experimental results. The most sophisticated dispersion model included argon solubility. The following equations describe the gas and liquid mass balance for the tracer when interphase mass transfer resistance is also considered:

$$D_G\frac{\partial^2 C_G}{\partial z^2} - \frac{U_G}{\epsilon_G}\frac{\partial C_G}{\partial z} + k_l a(HC_L - C_G) = \frac{\partial C_G}{\partial t} \tag{2}$$

$$D_L\frac{\partial^2 C_L}{\partial z^2} - \frac{\epsilon_G}{\epsilon_L}k_l a(HC_L - C_G) = \frac{\partial C_L}{\partial t} \tag{3}$$

The following boundary and initial conditions are used:

$$t = 0, \quad C_L = 0; \quad C_G = 0 \tag{4}$$

$$z = 0, \quad \frac{\partial C_L}{\partial z} = 0; \quad \frac{U_G}{\epsilon_G}C_G = D_G\frac{\partial C_G}{\partial z} + \frac{U_G}{\epsilon_G}\delta(t) \tag{5a}$$

$$z = L, \quad \frac{\partial C_L}{\partial z} = 0; \quad \frac{\partial C_G}{\partial z} = 0 \tag{5b}$$

It is assumed that the detector response is proportional to $\epsilon_L C_L(z,t) + \epsilon_G C_G(z,t)$. A similar model was presented and solved by Laplace transform by Van Vuuren (1988). Here we used a NAG (Numerical Algorithm Group) differential equation solver to get the time domain solution.

We assumed backmixing in the reactor gas space above the liquid level and that the outlet response is proportional to the exit mixing cup concentration for the gas. Radial uniformity of the tracer injection was adequate so that averaged responses of the detectors in the ring at a given elevation were used for comparison with model predictions.

Table 1: Parameter estimation using detectors at different elevations

	D_G (cm^2/s)	$k_l a$ (1/s)	H
30.5 cm	5789	0.1810	5.993
149.9 cm	6043	0.3016	4.676
337.8 cm	5626	0.1838	6.013
482.6 cm	5789	0.3055	5.032

There were three floating parameters: H, D_G, $k_l a$, while the measured mean values of gas and liquid holdup were used in the model together with the liquid dispersion coefficient determined earlier from tracer data.

The present model does not fare any better than the simpler models, as illustrated in Figure 3. Further attempts at curve fitting using different weights for the liquid and gas tracer concentrations in equation (9) for the detector response or accounting properly for the radial holdup distribution did not improve the consistency of the estimated parameters. This leads to the conclusion that the axial dispersion model with constant dispersion coefficients cannot match the observed gas tracer data.

Examination of the data at different elevations (Fig. 3) shows that the peak of the response shifts only slightly to larger times at higher elevations and that the spread of the curve does not increase much with elevation. This indicates that the response is mainly generated by the dissolved tracer in the liquid which is pretty well mixed. This is confirmed by the fact that the peak of the response occurs much later than the mean transit time for the undissolved gas, $\epsilon_G z/\overline{u}_G$. For example, for the detector at 149.9 cm elevation the mean gas transit time is less than 4 seconds while the response peak occurs at close to 20 seconds. The same pattern is observed for the detectors at all other elevations and at no detector is an early peak observed at the time corresponding to the mean transit time of the undissolved gas at that elevation. CARPT (Computer Automated Radioactive Particle Tracking) measurements (Devanathan, 1991) indicate that at conditions used in this study maximum liquid recirculation velocity could be of the order of 100 (cm/s). This implies that the tracer particle at the reactor centerline could transverse the whole liquid height in less than 6 seconds.

If we assume that the gas tracer input, instead of a delta function, is a response of a well mixed region given by:

$$f(t) = \frac{U_G}{\sqrt{U_G/(12\pi D_G)}} \exp\left(\frac{-(3-U_G t)^2}{12 D_G/U_G}\right) \tag{6}$$

This could be expected if rapid mixing and gas liquid transfer occurred in the sparger zone, then a good agreement between model predictions and data is possible as shown in Fig. 4. A consistent set of parameters is obtained (Table 1). Recomputing model predictions based on average parameter values still provides a good agreement between measured and modeled responses at all elevations. Theoretical justification for using this particular forcing function cannot be offered at present and work regarding this issue is in progress.

The parameter values listed in Table 1 are reasonable. The Henry's constant is close

to the value of calculated by Air Products, the volumetric mass transfer coefficient is close to the range of 0.1 to 0.2 (s^{-1}) predicted by most correlations (Fan, 1989), and the gas phase dispersion coefficient is well within the range of 1,000 to 20,000 (cm2/s) indicated by correlations (Fan, 1989). The gas phase Peclet number is of order one, and indicates that the gas phase is well mixed. This, however, may be an artifact of the model as liquid response dominates.

The overall gas phase tracer response in the outlet pipe are matched by assuming plug flow or complete backmixing in the gas space above the slurry level. It is found that the mixing pattern above the slurry level is bounded by the above two limits, but not close to either side.

CONCLUSIONS

The liquid, in our cigar shaped bubble column with the aspect ratio (L/D) of 10 and operated in churn turbulent regime, is well mixed. Complete mixing is achieved in about 90 seconds which is much shorter than the characteristic reaction time. Conversion predictions based on a well mixed compartment are therefore justified. The gas phase tracer runs cannot be interpreted satisfactorily based on the axial dispersion model. Very high backmixing of the dissolved gas is indicated but no conclusions can be reached regarding the flow pattern of the undissolved gas. The existence of symmetrical responses by detectors located in a ring at the same axial reactor elevation indicate presence of axial symmetry but is not sufficient proof of the lack of radial tracer concentration gradients. Only tracer injection close to the wall can reveal the existence of radial nonuniformities.

For the purpose of reactor modeling the tracer tests indicate that the industrial bubble column investigated here is close to a single well mixed tank which was the assumption made in calculating reactor performance.

NOMENCLATURE

A	area of the detector which can be reached by radiation, cm^2
a_1, b_1, a_2, b_2	coefficients for Berger equation, a_1 =1.30, b_1=0.027, a_2 =1.27, b_2=0.032
C_G, C_L	gas and liquid phase tracer concentrations, $mole/l$
D_G,D_L	gas and liquid phase dispersion coefficients, cm^2/s
d_A, d_M, d_S	radiation traveling distance in air, slurry and stainless steel, cm
$f(t)$	forcing function at the inlet.
H	Henry's law constant
L	liquid level in the bubble column, cm
N_t	total detector counting rate
k_la	mass transfer coefficient, $1/s$
S	source strength in a compartment = 1 (any units)
U_G	superficial gas velocity, cm/s
z_i	liquid tracer injection point, cm
δ	Dirac delta function.
ϵ	detector efficiency
ϵ_L, ϵ_G	liquid and gas holdups
μ_M, μ_S	attenuation coefficients, $\mu_M = 4.2 \times 10^{-2}$ $1/cm$, $\mu_S = 0.468$ $1/cm$

REFERENCES

Air Products and Chemicals Inc. and Chem Systems Inc. A Report to DOE Contract No. DE-AC22-87PC90005, August, 1990.

Devanathan, Doctoral Dissertation, Washington University, 1991.

Field, R. W.; Davidson, J. F. Trans IChemE, Vol. 58, 228, 1980.

Joseph, S.; Shah, Y. T. Can. J. Chem. Eng. Vol. 64, 380, June, 1986.

Nalitham, R. V.; Davies, O. L. Ind. Eng. Chem. Res. 1987, Vol. 26, 1059-1066.

Nicholas Tsoulfanidis. "Measurement and Detection of Radiation", Hemisphere Publishing Corp., 1983.

Shetty, S. A.; Kantak, M. V. AIChE J. Vol. 38, No. 7, 1013, 1992.

Tarmy, B. L.; Chang, M.; Coulaloglou, C. A.; Ponzi, P. R. I. Chem. E. Symposium Series, No. 87, 303, 1982.

Vermeer, D. J.; and Krishna, R. Ind. Eng. Chem. Process Des. Dev. Vol. 20, 475, 1981.

Van Vuuren, D. S. Chem. Eng. Sci. Vol. 43, No. 2, 213, 1988.

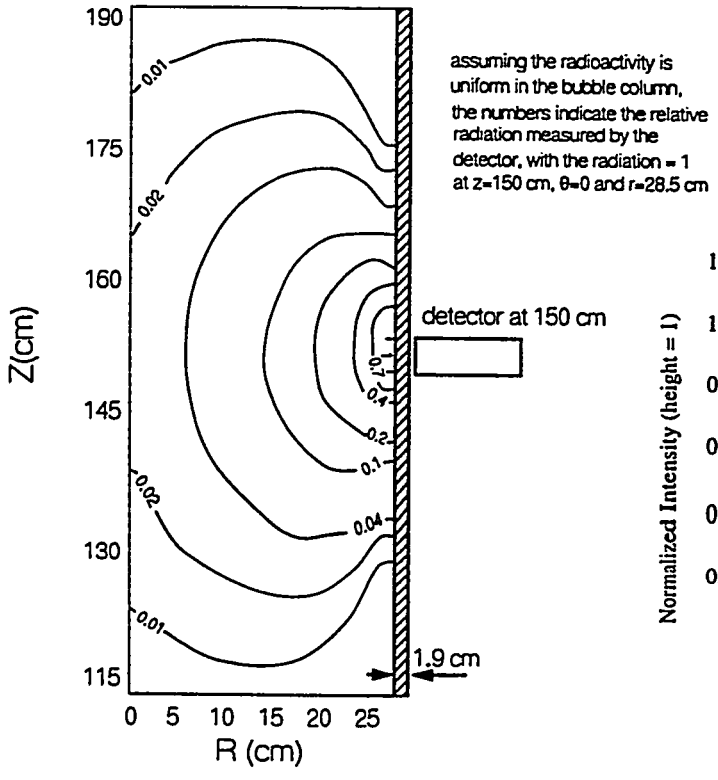

Figure 1: Schematic of the Radiation Measurement Calculation

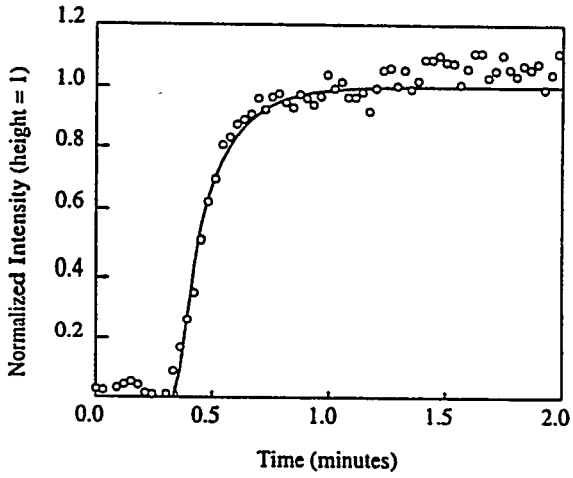

Figure 2: Time domain curve fitting for liquid tracer

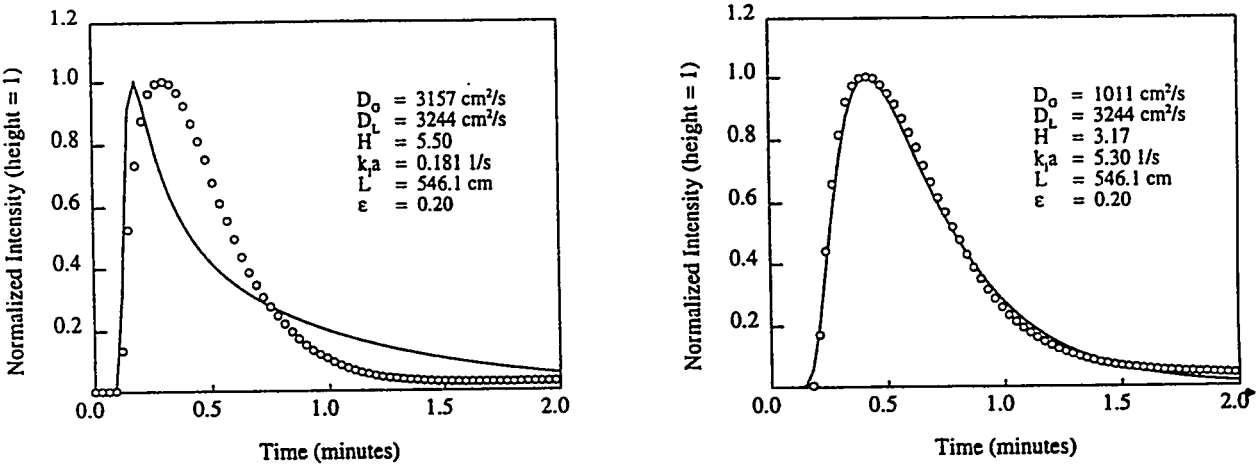

Figure 3: Time domain matching of the responses at different elevations using Dirac delta input function. A: 149.9 cm; B: 482.6 cm

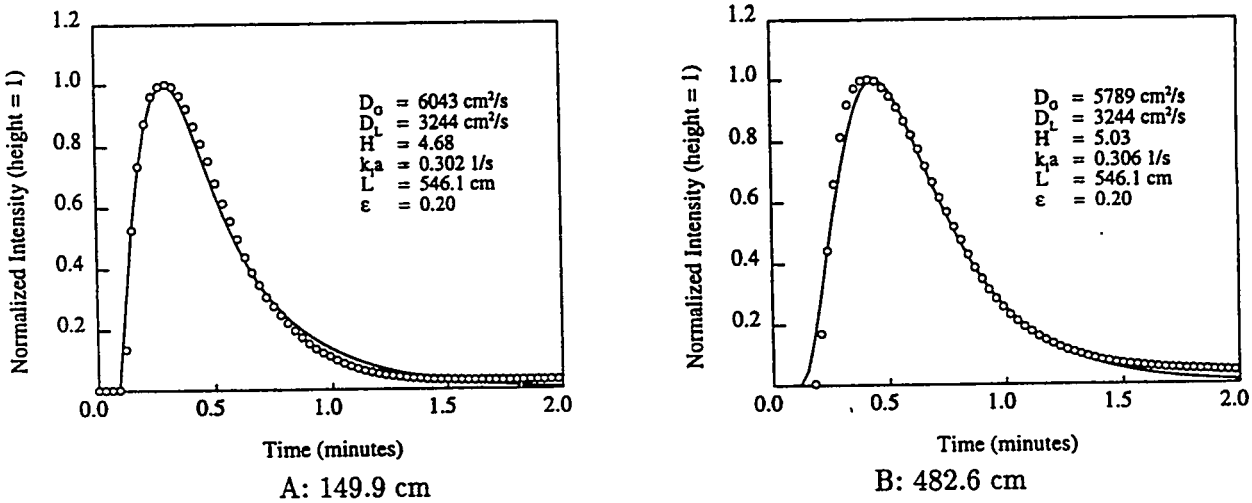

Figure 4: Time domain matching of the responses at different elevations using an exponential decaying input function. A: 149.9 cm; B: 482.6 cm

List of Figure Captions

Figure 1. Schematic of the Radiation Measurement Calculation.

Figure 2. Time Domain Curve Fitting for Liquid Tracer.

Figure 3. Time Domain Matching of the Responses at different Elevations Using Dirac Delta Input function.
A: 149.9 cm; B: 482.6 cm

Figure 4. Time Domain Matching of the Responses at Different Eleveations Using an Exponential Decaying Input Function.
A: 149.9 cm: B 482.6 cm